



HAL
open science

Realization of the optimal sizing of local hybrid photovoltaic and wind energy systems with load scheduling capacity

Majdi Saidi, Zhongliang Li, Seifeddine Ben Elghali, Rachid Outbib

► To cite this version:

Majdi Saidi, Zhongliang Li, Seifeddine Ben Elghali, Rachid Outbib. Realization of the optimal sizing of local hybrid photovoltaic and wind energy systems with load scheduling capacity. International Journal of Energy Research, inPress, 10.1002/er.7828 . hal-03599232

HAL Id: hal-03599232

<https://amu.hal.science/hal-03599232>

Submitted on 7 Mar 2022

HAL is a multi-disciplinary open access archive for the deposit and dissemination of scientific research documents, whether they are published or not. The documents may come from teaching and research institutions in France or abroad, or from public or private research centers.

L'archive ouverte pluridisciplinaire **HAL**, est destinée au dépôt et à la diffusion de documents scientifiques de niveau recherche, publiés ou non, émanant des établissements d'enseignement et de recherche français ou étrangers, des laboratoires publics ou privés.

Realization of the optimal sizing of local hybrid photovoltaic and wind energy systems with load scheduling capacity

Majdi Saidi, Zhongliang Li, Seifeddine Ben Elghali, Rachid Outbib

Abstract—Proper sizing of a local hybrid energy system is important to satisfy local power requirement and achieve low cost. This paper presents a sizing approach for a local photovoltaic (PV)/wind turbine (WT) hybrid energy system considering the capacity of local demand side management. In the approach, instantaneous energy consumption is modelled by analysing the power characteristics of various load types. Based on the model, local electricity load can be scheduled to minimize the electricity consumed from the utility grid. The system sizing is then formulated as a bi-level optimization problem, in which the down-level is dedicated to scheduling the energy consumption in a given energy generation profile, while the up-level is to seek for the optimal sizing of the hybrid energy system. Genetic and efficient global optimization algorithms are used respectively to solve the down-level and up-level optimization problems. A practical industrial case study is used to verify the sizing strategy. Different sizing configurations are realized and compared to demonstrate the benefits of the proposed approach.

Index Terms—Hybrid energy system sizing, demand side management, evolutionary algorithm, global optimization, mixed-integer optimization.

NOMENCLATURE

Subscript

<i>bat</i>	Battery
<i>c</i>	Controllable load
<i>c</i>	Cut-in
<i>e</i>	Electricity
<i>end</i>	End
<i>err</i>	Error
<i>f</i>	Fix load
<i>g</i>	Grid, global
<i>L</i>	Length of time
<i>l</i>	Load
<i>max</i>	Cut-off, maximum
<i>min</i>	Minimum
<i>new</i>	New
<i>p</i>	Production
<i>pv</i>	Photovoltaic
<i>pw</i>	PV/WT hybrid system
<i>r</i>	Rated
<i>s</i>	System
<i>start</i>	Start

wt Wind turbine

Variables

R	Correlation matrix
r	Correlation vector
x	Kriging model input
y	Kriging model output
\mathcal{T}	Period
δ	Self discharging rate
ϵ	Error of Gaussian process
η	Efficiency
$\hat{\cdot}$	Estimation of \cdot
μ	Mean of Gaussian process
Φ	Cumulative density function
ϕ	Probability density function
σ	Standard variance of Gaussian process
θ_k, p_k	Correlation parameters
A	Area
C	Cost
Cor	Correlation error
E	Energy
EI	Expected improvement
G	Solar radiation
I	Improvement
k	Discret time index
M	Dimension of Kriging model input
N	Number
P	Power
p	Price
s	Mean root square error
SOC	State of the charge
T	Control period
t	Time
T_g	Analysis duration
v	Speed

I. INTRODUCTION

It has been proven that renewable energy use could be promoted by increasing the decentralized energy generation proportion. Since the last two decades, increasing local renewable energy system installations have been prompted by policy encouragement and system cost decrease [1]. The local energy system is often hybridized with different energy sources and combined with energy storage units (ESUs) to realize a secure and flexible energy supply [2].

From power consumers' point of view, the investment of local hybrid energy systems could be attractive for economic

All the authors are with the LIS Lab (UMR CNRS 7020), Aix-Marseille University, 13397 Marseille Cedex 20, France (e-mail: zhongliang.li@lis-lab.fr; majdi.saidi@lis-lab.fr; seifeddine.benelghali@lis-lab.fr; rachid.outbib@lis-lab.fr). M. Saidi is also with Energy Mechanical Building company, 13420 Gemenos, France.

and ecological reasons. For potential investors, system sizing plays a crucial role at the feasibility analysis stage. Besides, a well sized local energy system could be beneficial to supply more secure power, higher electricity quality and system efficiency [3]. Various variables can be taken into account for sizing a local hybrid energy system, such as those quantify power security level, economic and ecological impacts. In most cases, depending on the specific requirements, the system sizing is formulated as a constrained optimization problem [4]. Different hybrid energy sizing formulation and resolution methods can be found in recent review papers [5][6][7].

For sizing a hybrid energy system, various factors need to be considered including the ones characterize reliability, economic, environmental and social impacts [7]. In different sizing optimization formulations, the power balance of generation and consumption sides is one of the most important elements. As a reliability indicator, the power balance has been considered as either a criterion or a constraint and formed mathematically in various forms. For instance, loss of power supply probability (LPSP), defined as the percentage of power supply that the concerned energy system is not able to satisfy the load demand, has been widely used to quantify the power balance performance. In most studies, the LPSP is applied as a constraint in the way that the LPSP of the concerned system must be less than a preset value [8][9][10]. In other formulations, the LPSP is considered as an objective to minimize [11][12]. In the latter case, the LPSP concept is often considered together with other factors in a multi-objective sizing problem [13]. Similar to the LPSP concept, other quantities, such as loss of load probability and loss of energy expected, have also been proposed to evaluate the power balance of hybrid energy systems and used for sizing. These indicators of power balance have been explained and compared in recent review papers [7][5].

Sizing a local hybrid energy system is specific to the characteristics of the concerned energy consumer. To analyse and evaluate the power balance using the afore-mentioned indicators, the specific load power profiles and/or the historical consumption traces are required [7][5]. The system size is thus dependent on the load properties of the concerned consumer.

With the development of smart-grids technology, it is becoming interesting to plan some local loads to adapt to the energy generation characteristics and realize effective demand side management (DSM) [14]. In addition to the management of energy generation side, the integration of DSM offers more potential to improve the performance of distributed hybrid energy systems in terms of reduced system operation costs, electricity costs, and improved power supply security [15]. During the last years, several DSM strategies have been proposed for local hybrid energy systems. For instance, in [16], a load scheduling approach is proposed to store excess renewable energy as industrial products. Much more works are focused to the load planning for domestic applications [17][18]. More systematic insights of DSM can be referred in the review paper [19][20][21].

The load scheduling is dependent on the property of generated energy whose capacity and characteristics are determined largely by the system size. For an energy system, sizing and

load scheduling are therefore correlated and influence each other. However, in most of the sizing methods, the flexibility of load scheduling is not considered explicitly, but only treated by adding an uncertain factor of load [15]. In other works, load scheduling is often conducted for a roughly sized system [22]. As the sizing and load scheduling proceed separately, the system size could be improper to release fully the advantages of load scheduling.

The main objective of this work is to propose a novel optimal sizing strategy, including both sizing problem formulation and resolution, for the electricity consumers in consideration of the load flexibility. Two representative users with such flexibility are metallurgical and equipment manufacturing industries [23]. The preliminary idea of the strategy was presented in [24], while this work has enhanced the involved methodologies and results. The proposed sizing strategy consists in adapting the load scheduling as much as possible to the available locally generated energy for an electricity consumer.

The sizing of the local energy system together with the load scheduling is formulated as a deterministic static bi-level optimization problem. On the down-level, the load power characteristic in function of different load types is modelled firstly. Then, the load scheduling subject to one load variation cycle is realized by minimizing the electricity supplied from the local power grid. The up-level optimization is formulated outside the load scheduling operation and dedicated to the system sizing.

The novel formulation of sizing problem necessities novel resolution methods. Technically, to find a solution to this problem necessitating a large time for computation, a heuristics solution genetic algorithm (GA) and Bayesian optimization method efficient global optimization (EGO) are adopted respectively in the two levels to obtain the final optimal sizing results. To illustrate the proposed approach, a real industrial case is considered. In the case, a hybrid energy system composed by photovoltaic (PV) panels, wind turbines (WT) and optional ESUs is designed for an industrial manufacturer to compensate the consumption of electricity from the utility grid.

The contributions of this work can be summarized as follows:

- Modelling and scheduling methods are proposed for industrial energy consumers.
- Bi-level optimization is formulated for the system sizing integrated with load scheduling. GA and EGO algorithms are proposed to solve the bi-level problem.
- Effectiveness of the strategy is validated through comparative studies.

The remaining paper is organized in following way: In Section II, the model of the PV/WT hybrid energy system and the design criterion is presented. The system design with ESUs is also introduced in this section. Then, load modelling and scheduling procedures are described in Section III. The bi-level optimization framework and the algorithms are presented in Section IV. Following that, the results of the case study are provided and discussed in Section V. Finally, Section VI concludes the proposed work.

II. SYSTEM MODELLING AND DESIGN CRITERIA

Throughout the paper, we will use the following notations. The time is denoted t and is assumed to be belonging to a period $\mathcal{T} = (0, T_g)$ where T_g designates the global duration of the analysis, i.e. the life cycle of the hybrid energy system. In the sequel, we will use the integer interval notation, namely, for two integers $a < b$, $\llbracket a, b \rrbracket$ will denote the set $\{a, a + 1, \dots, b\}$.

A. System modelling

To size the hybrid energy system properly, the power flow should be analysed firstly. The structure of the studied hybrid energy system is illustrated in Fig. 1. To simplify the system installation and maintenance, ESUs will be optionally installed in this system. To achieve optimal efficiency, it is supposed that the energy on both supply and demand sides can be managed and with bidirectional communication.

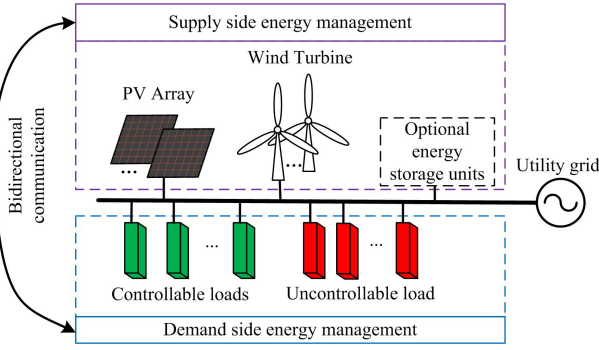


Fig. 1. Diagram of the PV/WT hybrid energy system.

Considering that a maximum power point track regulator is used for the PVs, the power generated by a PV panel $P_{pv}(t)$ at time $t \in \mathcal{T}$ can be modelled as a linear function of radiation [25], as

$$P_{pv}(t) = G(t)A_{pv}\eta_{pv} \quad (1)$$

where $G(t)$ is the solar radiation at $t \in \mathcal{T}$ depending on local climatic condition. A_{pv} and η_{pv} are respectively the PV panel surface and efficiency, which depends on the characteristics of the used PV.

$P_{wt}(t)$, power generated by a WT, is modelled using a piece-wise function of the wind speed $v(t)$ [26]:

$$P_{wt}(t) = \begin{cases} 0, & v(t) < v_c \\ P_r \frac{v(t)^3 - v_c^3}{v_r^3 - v_c^3}, & v_c \leq v(t) < v_r \\ P_r, & v_r \leq v(t) < v_{max} \\ 0, & v(t) \geq v_{max} \end{cases} \quad (2)$$

where P_r is the rated power of the WT; v_c , v_r , and v_{max} are named cut-in, nominal and cut-off speeds whose values are dependent on the WT characteristics.

Given N_{pv} and N_{wt} , the numbers of PV panels and WTs, the instantaneous power generated by the PV/WT hybrid energy system $P_{pw}(t)$ is calculated, for $t \in \mathcal{T}$, as

$$P_{pw}(t) = N_{pv}P_{pv}(t) + N_{wt}P_{wt}(t) \quad (3)$$

B. Energy management

ESUs are optionally installed in the hybrid energy system. Here, we consider using Li-ion batteries as ESUs. The variation of the state of charge (SOC) of the batteries is modelled as follows

$$SOC(t+T) = SOC(t)(1-\delta) + P_{bat}(t)T\eta_{bat}(P_{bat})^{sign(P_{bat})}/E_{bat,max} \quad (4)$$

where δ is battery self discharging rate; $P_{bat}(t)$ is the charging power and the negative $P_{bat}(t)$ denotes that battery is in discharging operation; $E_{bat,max}$ is the maximum energy that the battery can store; η is the efficiency of the battery.

With the ESUs, the energy flow is managed using basic rules. Given the parameters of an energy storage unit, the energy management rules are summarized in Algorithm 1. A main principle adopted for establishing this algorithm consists of using first the available energy from renewable sources. With the energy management rules, the power supplied by utility grid P_g can be determined. It should be noted that the average battery capacity is used to consider the effect of battery degradation. In the case that there is no ESUs in the hybrid system, $P_g(t)$ can be calculated as follows

$$P_g(t) = \begin{cases} P_l(t) - P_{pw}(t), & P_l(t) > P_{pw}(t) \\ 0, & P_l(t) \leq P_{pw}(t) \end{cases} \quad (5)$$

where P_l is the load power. It should be noted that, in this study, the local generated power is not allowed to feed the power grid, but only used for the local energy use.

C. Cost analysis

The whole cost during the life cycle of the system C_g is composed by the system cost C_s and electricity cost C_e , as

$$C_g = C_s + C_e \quad (6)$$

where the system cost consists of the costs related to PVs, WT and batteries, as

$$C_s = p_{pv} N_{pv} + p_{wt} N_{wt} + p_{bat} N_{bat} \quad (7)$$

where p_{pv} , p_{wt} , p_{bat} are the unit costs of PV, WT and battery which cover the initial costs, including acquisition and installing costs, operating & maintenance and replacement costs.

The electricity cost corresponding to the concerned system life cycle is calculated as follows

$$C_e = p_e \int_0^{T_g} P_g(\tau) d\tau \quad (8)$$

where p_e is the price of electricity from power grid.

The objective of system sizing is to minimize the total cost C_g by finding the optimal combination of hybrid system components, namely N_{pv} , N_{wt} and N_{bat} .

Algorithm 1 Rule-based supply side energy management strategy.

Require: $SOC(t)$ (battery state of charge), $P_{pw}(t)$, $P_l(t)$;
Ensure: $SOC(t+T)$, $P_{bat}(t)$, $P_g(t)$

- 1: **if** $P_{pw}(t) > P_l(t)$ **then**
- 2: $P_g(t) = 0$
- 3: **if** $SOC(t) < SOC_{max}$ **then**
- 4: **if** $P_{pw}(t) - P_l(t) < P_{bat,max}$ **then**
- 5: $P_{bat}(t) = P_{pw}(t) - P_l(t)$
- 6: **else**
- 7: $P_{bat}(t) = P_{bat,max}$
- 8: **end if**
- 9: **else**
- 10: $P_{bat}(t) = 0$
- 11: **end if**
- 12: **else**
- 13: **if** $SOC(t) > SOC_{min}$ **then**
- 14: **if** $P_{pw}(t) - P_l(t) > P_{bat,min}$ **then**
- 15: $P_{bat}(t) = P_{pw}(t) - P_l(t)$
- 16: $P_g(t) = 0$
- 17: **else**
- 18: $P_{bat}(t) = P_{bat,min}$
- 19: $P_g(t) = P_l(t) - P_{pw}(t) + P_{bat}(t)$
- 20: **end if**
- 21: **else**
- 22: $P_{bat}(t) = 0$
- 23: $P_g(t) = P_l(t) - P_{pw}(t) + P_{bat}(t)$
- 24: **end if**
- 25: **end if**
- 26: Update $SOC(t+T)$ according to (5).

III. LOAD MODELLING AND SCHEDULING

For a hybrid energy system equipped with ESUs, the overall characteristics of generated power can be adjusted to match the load power characteristics by manipulating the charging and discharging power of the ESUs. In this study, to reach the equivalent effect, the effort is made to adjust the load power aiming to match the characteristics of energy generation.

In this work, a framework of industrial application is considered. However, the proposed approach can be used for other applications. First, the electricity consumption is modelled to achieve load scheduling. The different loads can be recognized as controllable loads related to the production tasks, and uncontrollable or fixed ones. In this work, the strategy consists in adjusting the controllable part of the load and the analysis is focused on a production cycle.

As shown in Fig. 2(a), a production cycle can be subdivided to N_p time slots. At each time slot, the whole power $P_l(k)$ ($k \in \llbracket 1, N_p \rrbracket$) can be considered as the sum of two quantities, namely,

$$P_l(k) = P_f(k) + P_c(k), \quad (9)$$

where $P_c(k)$ ($k \in \llbracket 1, N_p \rrbracket$) is the power sum of all controllable loads, as

$$P_c(k) = \sum_{i=1}^{N_c} P^{(i)}(k), \quad (10)$$

where $P^{(i)}$ is the power i th controllable load and N_c denotes the number of controllable loads. In Fig. 2(a), $N_c = 2$.

For $i \in \llbracket 1, N_p \rrbracket$, the i th load is started at k_i th time slot and lasts for L_i time slots. The power of the i th task is therefore

$$P^{(i)}(k) = \begin{cases} P_r^{(i)}, & k \in \llbracket k_i, k_i + L_i - 1 \rrbracket \\ 0, & k \in \llbracket 1, k_i - 1 \rrbracket \cup \llbracket k_i + L_i, N_p \rrbracket \end{cases} \quad (11)$$

where $P_r^{(i)}$ is the average power of the i th load.

L_i is considered as constant satisfying $L_i \leq N_p$. The load power $P_l(k)$ is then a function of starting time of each task k_i ($i \in \llbracket 1, N_c \rrbracket$).

It should be noted that the powers $P_r^{(i)}$ and durations L_i ($i \in \llbracket 1, N_c \rrbracket$) of different controllable and fixed loads can be identified by analysing the power consumption of each individual production task. In the focused production cycle, it is considered that there are always redundant premier materials for different tasks. With redundant premier materials, different tasks can be carried out independently.

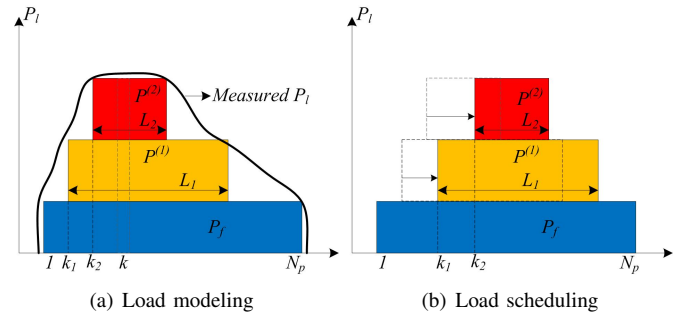


Fig. 2. Schematic diagram of load modelling and scheduling.

With the identified load model, the power curve can be configured by assigning the starting times k_i to controllable loads, as shown in Fig. 2(b). In this study, the load is scheduled to sufficiently use local generated energy and minimize the energy supplied by the power grid. The energy from the power grid is

$$E_g = \sum_{k=1}^{N_p} P_g(k)T \quad (12)$$

where T is the control period. In the case that there is no ESUs in the hybrid system, $P_g(k)$ can be calculated as follows

$$P_g(k) = \begin{cases} P_l(k) - P_{pw}(k), & P_l(k) > P_{pw}(k) \\ 0, & P_l(k) \leq P_{pw}(k) \end{cases} \quad (13)$$

where the power generated, denoted as $P_{pw}(k)$, $k \in \llbracket 1, N_p \rrbracket$, is considered known. E_g is therefore dependent on $P_l(k)$, which is finally a function of $k_i \in \llbracket 1, N_p \rrbracket$. Therefore, the load scheduling problem seeks to minimize E_g by varying k_i ($i \in \llbracket 1, N_c \rrbracket$).

IV. OPTIMAL SIZING STRATEGY VIA BI-LEVEL OPTIMIZATION

As shown in Fig. 3, the optimal sizing is realized through a bi-level optimization procedure [24]. The down-level and up-level optimizations are respectively dedicated to load scheduling and system sizing.

In the down-level optimization, the minimized electricity cost $C_e^{(m)}$, which is proportional to the energy supplied by grid $E_g^{(m)}$, can be obtained after conducting load scheduling for production cycle m . The same load scheduling procedure will be adopted for each production cycle in the concerned period T_g .

In the up-level optimization, the whole cost C_g , which could quantify the long-term profit, is used for evaluating a sizing option. In the concerned period, multiple (N_g) production cycles will be handled with load scheduling actions. It should be noted that the load scheduling is carried out independently for each production cycle such that the variation among different production cycles can be taken into account.

Solving the optimization problems separately in the two levels is beneficial since the overall problem can be decomposed into sub optimization problems with smaller scales in terms of variable number. In the sequel, the optimization problems and the corresponding solvers will be introduced respectively for the two levels.

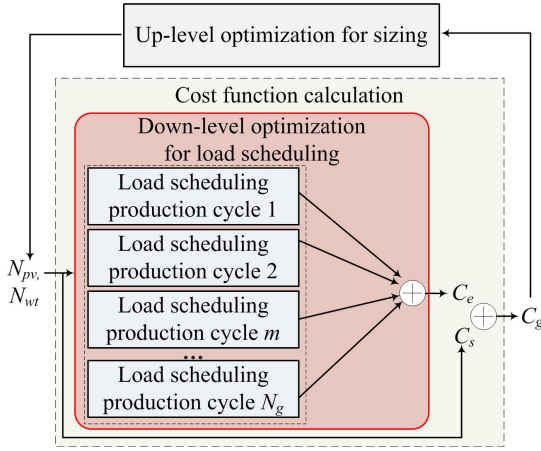


Fig. 3. Schematic of the proposed sizing approach based on bi-level optimization.

A. Load scheduling in down-level optimization

The objective at this level is to minimize energy consumption from the power grid by scheduling the controllable loads. The starting times k_i are constrained by the stating time hour k_{start} , end time hour k_{end} and their durations L_i . The load scheduling is formulated as a mixed integer optimization problem.

$$\begin{aligned} \min E_g^{(m)}(k_1, k_2, \dots, k_{N_c}) \\ \left\{ \begin{array}{l} k_i \in [k_{start}, k_{end} - L_i] \\ i \in [1, N_c] \end{array} \right. \end{aligned} \quad (14)$$

To solve the problem using exhaustive search, the computational complexity is $O((k_{end} - k_{start})^{N_c})$. In the case where the number of controllable loads N_c is large, the traditional approaches such as branch and bound, are meant for a small number of variables and often yield approximate results [27]. In this study, GA is adopted to resolve the down-level optimization and reduce the computational time [28]. As GA has been successfully applied in many practical cases, the

implementation of GA will not be depicted in this paper. The details of the realization of GA can nevertheless be found in [29]. A detailed Matlab implementation example can also be found in [30].

B. System sizing in up-level optimization

In the concerned period for sizing, the total electricity cost C_e is the sum of the costs for all involved production cycles, as

$$C_e(N_{pv}, N_{wt}) = \sum_{m=1}^{N_g} C_e^{(m)} = p_e \sum_{m=1}^{N_g} E_g^{(m)} \quad (15)$$

where p_e is the electricity price.

The up-level optimization is formulated as

$$\begin{aligned} \min C_g(N_{pv}, N_{wt}) &= C_s(N_{pv}, N_{wt}) + C_e(N_{pv}, N_{wt}) \\ \left\{ \begin{array}{l} N_{pv} \in [N_{pv, min}, N_{pv, max}] \\ N_{wt} \in [N_{wt, min}, N_{wt, max}] \end{array} \right. \end{aligned} \quad (16)$$

where C_s and C_e are calculated respectively using (7) and (15). The linkage between up-level and down-level optimizations lies in the calculation of electricity cost C_e . For this term, multiple down-level optimizations have to be realized in each calculation of C_g , which is computationally heavy. To alleviate the computing burden, the objective function calls should be reduced in the optimization algorithm. EGO is adopted in the up-level optimization for this purpose. The principle of EGO is to use a surrogate model instead of the original objective function. By optimizing the less costly surrogate model instead of the original cost function, the computing time can be reduced.

In our case, denoting $\mathbf{x} = [N_{pv}, N_{wt}]$, the Kriging model mimics the cost function $y = C_g(\mathbf{x})$ in (15) as a Gaussian process. Based on a set of input points $\mathbf{X} = [\mathbf{x}(1); \mathbf{x}(2); \dots; \mathbf{x}(n)]$ and their function values $\mathbf{y} = [y(1); y(2); \dots; y(n)]$, a Kriging model can be built as:

$$y(\mathbf{x}) = \mu + \epsilon(\mathbf{x}) \quad (17)$$

where μ is the mean of the Gaussian process. ϵ is the normal distributed error with mean zero and variance σ^2 .

The correlation error between $\epsilon(\mathbf{x}^{(i)})$ and $\epsilon(\mathbf{x}^{(j)})$ is a function of their distance, as

$$Cor(\epsilon(\mathbf{x}^{(i)}), \epsilon(\mathbf{x}^{(j)})) = \exp\left(-\sum_{k=1}^M \theta_k |x_k^{(i)} - x_k^{(j)}|^{p_k}\right) \quad (18)$$

where M is the dimension of the input variables (2 in our case), θ_k and p_k ($k = 1, 2, \dots, M$) are parameters to be determined. Together with μ and σ , $2M + 2$ parameters need to be estimated. The parameters can be found by maximizing the likelihood of the samples [31]. Given the correlation parameters θ_k and p_k for $k = 1, 2, \dots, M$, μ and σ can be deduced in closed form, as

$$\hat{\mu} = \frac{\mathbf{1}^T \mathbf{R}^{-1} \mathbf{y}}{\mathbf{1}^T \mathbf{R}^{-1} \mathbf{1}} \quad (19)$$

$$\hat{\sigma} = \frac{(\mathbf{y} - \mathbf{1}\hat{\mu})^T \mathbf{R}^{-1} (\mathbf{y} - \mathbf{1}\hat{\mu})}{n} \quad (20)$$

where \mathbf{R} denotes a $n \times n$ matrix whose (i, j) entry is $Cor(\epsilon(\mathbf{x}^{(i)}), \epsilon(\mathbf{x}^{(j)}))$, $\mathbf{1}$ is n -dimensional vector with all entries 1.

The prediction of an unknown point x and the mean squared error s^2 of the prediction can be calculated using the Kriging model

$$\hat{y}(\mathbf{x}) = \hat{\mu} + \mathbf{r}^T \mathbf{R}^{-1}(\mathbf{y} - \mathbf{1}\hat{\mu}) \quad (21)$$

$$s^2(\mathbf{x}) = \sigma^2 \left[1 - \mathbf{r}^T \mathbf{R}^{-1} \mathbf{r} - \frac{(1 - \mathbf{1}^T \mathbf{R}^{-1} \mathbf{r})}{\mathbf{1}^T \mathbf{R}^{-1} \mathbf{1}} \right] \quad (22)$$

where \mathbf{r} denotes the n -vector with i th entry $r_i = Cor(\epsilon(\mathbf{x}), \epsilon(\mathbf{x}^{(i)}))$.

The identified Kriging model is validated by carrying out a leave-one-out cross-validation procedure. Specifically, given a data set (\mathbf{X}, \mathbf{y}) , the predicted output $\hat{y}(i)$ of a test sample $\mathbf{x}(i)$ is calculated through the model identified using the remaining $n - 1$ samples. Following that, the number of standard errors that the actual value is above or below the predicted value $N_{err}(\mathbf{x}(i))$ is computed as

$$N_{err}(\mathbf{x}(i)) = \frac{y(i) - \hat{y}(i)}{s} \quad (23)$$

The model is considered to be valid if $N_{err}(\mathbf{x}(i))$ is in interval $[-3, 3]$. More details on model validation can be found in [31].

The real cost function value $C_g(\mathbf{x})$ of \mathbf{x} follows Gaussian distribution with mean $\hat{y}(\mathbf{x})$ and variance $s^2(\mathbf{x})$. The improvement of this point beyond the best observed value y_{min} is then

$$I(\mathbf{x}) = \max(y_{min} - C_g(\mathbf{x}), 0) \quad (24)$$

Based on the distribution of $C_g(\mathbf{x})$, the expected improvement value can be derived as [31]

$$EI(\mathbf{x}) = (y_{min} - \hat{y}(\mathbf{x})) \Phi \left(\frac{(y_{min} - \hat{y}(\mathbf{x}))}{s(\mathbf{x})} \right) + s(\mathbf{x}) \phi \left(\frac{(y_{min} - \hat{y}(\mathbf{x}))}{s(\mathbf{x})} \right) \quad (25)$$

where $\Phi(\mathbf{x})$ and $\phi(\mathbf{x})$ are the cumulative density function and probability density function of the normal distribution respectively. In the EGO algorithm, the sample with the maximum EI value, which is considered as the most probable solution, is evaluated and added to the sample set. The procedure is repeated until the maximum EI is less than a prescribed value (e.g., $0.01y_{min}$). The whole EGO process is summarized in Algorithm 2. More details on EGO theoretical deduction can be found in [31] [32] [33].

V. CASE STUDY

In this section, the proposed sizing strategy is applied to one industrial case. In the case, a PV/WT hybrid energy system with optional ESU is designed. It should be noted that the sizing strategy could also be used for other cases where the load can be partially or fully scheduled.

First, we introduce technical parameters used in this study. Second, we propose four scenarios for distinguishing different cases according to the presence or not of storage system and with or without a scheduling procedure. Particularly,

Algorithm 2 EGO algorithm for up-level optimization.

Require:

- 1: Initialize design set (\mathbf{X}, \mathbf{y}) , set algorithm threshold ϵ_{EI}
- 2: Estimate parameters of Kriging model: $\hat{\mu}$, $\hat{\sigma}$, \hat{y} , and s according to (19), (20), (21) and (22)
- 3: Calculate EI for all possible \mathbf{x} according to (25)

Ensure:

- 1: **while** $\max EI(\mathbf{x}) > \epsilon_{EI}$ **do**
- 2: $\mathbf{x}_{new} = \operatorname{argmax} EI(\mathbf{x})$
- 3: $\mathbf{y}_{new} = C_g(\mathbf{x}_{new})$
- 4: $\mathbf{X} \leftarrow \mathbf{X} \cup \mathbf{x}_{new}$
- 5: $\mathbf{y} \leftarrow \mathbf{y} \cup \mathbf{y}_{new}$
- 6: $y_{min} = \min(\mathbf{y})$, $\mathbf{x}_{min} = \mathbf{x} : C_g(\mathbf{x}) = y_{min}$
- 7: Estimate parameters of Kriging model: $\hat{\mu}$, $\hat{\sigma}$, \hat{y} , and s according to (19), (20), (21) and (22)
- 8: Calculate EI for all possible \mathbf{x} according to (25)
- 9: **end while**

the proposed bi-level optimization based sizing strategy is applied for the third scenario. The performance of the bi-level optimization solver combining GA and EGO is evaluated. Third, we give a comparative analysis.

A. Parameters of the studied case

The technical and economical parameters of the PV panel, WT and battery selected from the market are summarized in Table I. The PV, WT and battery installing capabilities are constrained by the available space and the installation requirements. By evaluating the studied case, the maximum number of PV panels $N_{pv,max}$, WTs $N_{wt,max}$ and batteries $N_{bat,max}$ are respectively 371, 6 and 40.

TABLE I
TECHNICAL AND ECONOMICAL PARAMETERS OF THE SYSTEM COMPONENTS

	Variable	Value
PV panel	A_{pv}	1.64 m ²
	η_{pv}	0.17
WT	v_c	10 m/s
	v_r	12.5 m/s
	v_{max}	20 m/s
	P_r	4 kW
Battery	$E_{bat,max}$	4.92 kWh
	δ	0.0002
	$P_{bat,max}$	1.674 kW
	$P_{bat,min}$	-1.674 kW
	η_{bat}	0.98
Price	p_{pv}	220 €/unit
	p_{wt}	3080 €/unit
	p_{bat}	1100 €/unit
	p_e	0.065 €/kWh

The production cycle is considered as one workday. During the product fabrication process, 12 tasks numbered from 1 to 12 need to be scheduled. The electricity consumers for the 12 tasks and their nominal powers are listed in Table II. By analysing the operation process in each task, the average powers and the durations of 12 production tasks are

listed in Table III. In addition to the loads corresponding the product fabrication activities, there are also some regular electricity consumption relating to lighting, office work, air condition, etc. The power composition of different loads and the measured power in one workday are shown in Fig. 4. It is seen that the identified model is able to represent the real power consumption characteristics. In the concerned production cycle, the energy share of the controllable loads accounts for 36%.

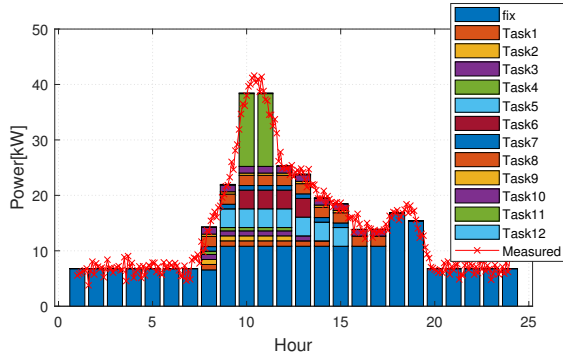


Fig. 4. Measured and modelled load power during one production cycle.

In the studied case, it is considered that the same production cycle is repeated from every Monday to Friday each week, while constant load of 3 kW is considered in weekend, i.e., Saturday and Sunday.

TABLE II

LIST OF INVOLVED ELECTRICITY CONSUMERS AND THEIR POWERS

Load	Number	Power per unit (kW)
Grinder	3	1.2
Perseuse	1	0.5
Pinter	4	0.2
Soldering station	1	2.45
Welding machine	2	4.5
Overhead crane 1	1	2.7
Overhead crane 2	1	5.5
Workshop extractor	2	1.5
Fan	1	1.5
Electric saw	1	1.1
Paint extractor	1	7.5
Compressor	1	6

The historical solar radiation and wind speed data of the concerned geographical position are collected. The system life cycle T_g of 20 years is used to calculate the global cost.

B. Scenario 1: system sizing with neither energy storage nor load scheduling

In this scenario, the sizing of the system is carried out with neither energy storage nor load scheduling. The load powers are considered to be identical. Given a combination N_{pv} and N_{wt} , the value of the cost function C_g in (6) is simple to calculate. The optimal sizing can be found through an extensive search of all possible sizing options. The number of combinations N_c is dependent on the maximum installation capacities, as

$$N_c = (N_{PV,max} + 1)(N_{wt,max} + 1) \quad (26)$$

By deploying the extensive search algorithm, the optimal PV panel number $N_{pv} = 44$ and WT number $N_{wt} = 4$ are obtained. With this sizing option, the total cost C_g is 1.016×10^5 €, and the system cost $C_s = 3.400 \times 10^4$ €, electricity cost $C_e = 6.758 \times 10^4$.

For comparison, the electricity cost is 1.258×10^5 € if the system is not installed. It is therefore economically beneficial to install the local PV/WT hybrid system.

The locally generated and consumed powers during one year and one specific production cycle are shown in Fig. 5. It is noticed that the power generation and consumption are often mismatched. For instance, in the period shown in the magnified figure, the energy demanded is intensive in the morning while the generation peak is in the afternoon. The locally generated energy is not used sufficiently.

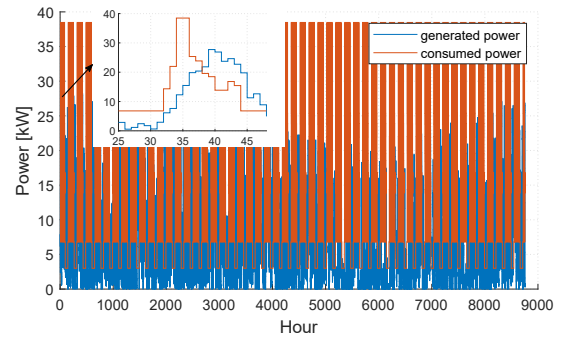


Fig. 5. Comparison of the generated and load powers with neither energy storage nor load scheduling.

C. Scenario 2: post load scheduling with a pre-designed system without energy storage

In this scenario, load scheduling is carried out with the same sizing option in the last scenario. As stated in Section IV, GA is deployed to realize load scheduling for all the production cycles within the system life-cycle. Regarding the problem shown in (14), the starting time hour k_{start} and the end time hour k_{end} are set respectively as 7 and 20 considering the staffs' working time.

After the load scheduling operation, C_e is reduced to 6.385×10^4 €. The generated and load powers for one production cycle are shown in Fig. 6. By moving the controllable loads, the power generation and consumption are matched better than the previous scenario without load scheduling.

D. Scenario 3: system sizing with load scheduling without energy storage

As presented in Section IV, the optimal sizing considering load scheduling capability can be achieved via the proposed bi-level optimization. For the cost function calculation of each sizing option, i.e., the combined numbers of PV panels and WTs, GA has to be run for all production cycles, which is time-consuming. In our case, the load scheduling for all production cycles in 20 year, which accounts for 5420 workdays, takes about 1 min. If the extensive research is adopted, the

TABLE III
AVERAGE DURATIONS AND POWERS OF THE PRODUCTION TASKS

Task index	1	2	3	4	5	6	7	8	9	10	11	12
L_i/h	7	5	6	5	7	4	8	10	8	10	2	7
$P_r^{(i)}/kW$	0.98	0.90	0.90	0.60	3.38	3.38	0.83	1.84	0.42	1.20	13.13	0.13

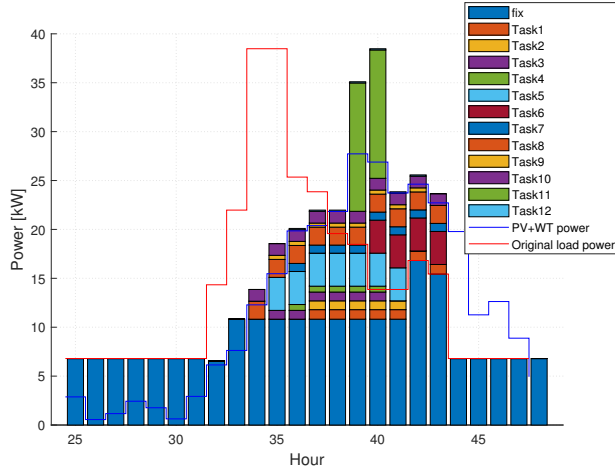


Fig. 6. Comparison of the generated power and load power with the pre-designed system. Red line: original load power; Blue line: generated power; Colourful blocks: scheduled power.

calculation time for all possible sizing combinations will be about 2604 mins. This is considered unsupportable especially when some parameters of the installed system change and the sizing has to be re-conducted. By using the EGO algorithm for the up-level optimization, the optimum can be found with a smaller number of cost function calculations.

As indicated in Algorithm 2, 10 samples are randomly sampled from all sizing combinations and formed as the initial design set. A leave-one-out cross-validation is then carried out over the initial design set. The $N_{err}(\mathbf{x}(i))$ values in (23) is shown in Fig. 7. As all $N_{err}(\mathbf{x}(i))$ values are within the interval $[-3, 3]$, the identified Kriging model is thus validated.

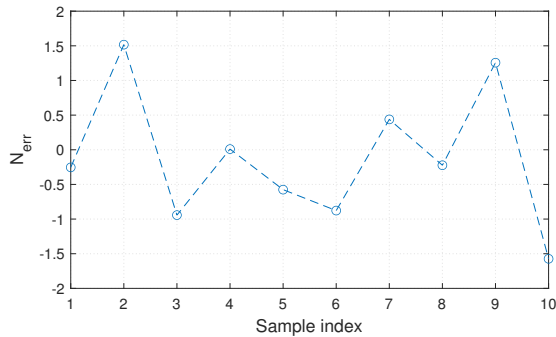
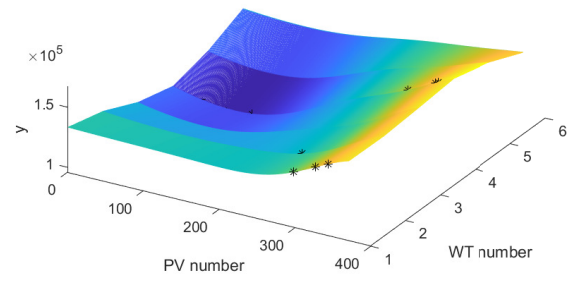
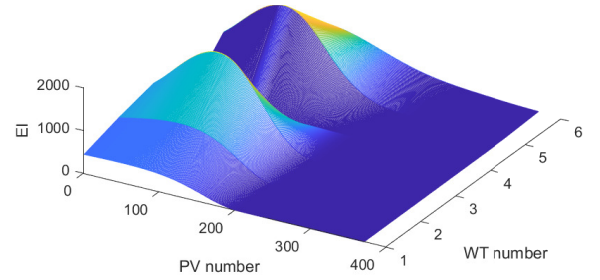


Fig. 7. N_{err} values of all samples in a leave-one-out cross-validation test.

Starting with the initial design set, the optimal sizing option can be found by implementing Algorithm 2. The parameter ϵ is set as $0.0001y_{min}$. The Kriging function surfaces and the



(a) Kriging function surface and samples in design set.



(b) Expected improvement.

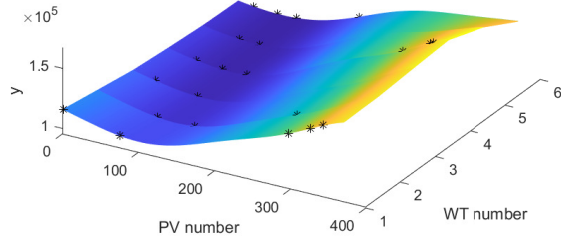
Fig. 8. Initial Kriging function surface and EI .

expectation improvement EI before and after the while loop are shown respectively in Fig. 8 and 9. It can be seen that the Kriging function and EI surfaces evolve with the increase of sample number in design set. The final EI values all decrease to a low level.

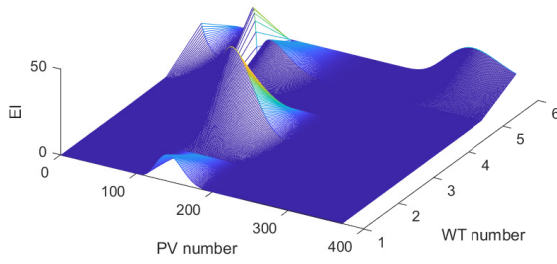
To evaluate the performance of up-level optimization algorithm, the EGO is implemented for 5 times with different random initial design sets. The minimum function output y_{min} and the maximum expected improvement $max(EI(\mathbf{x}))$, shown in Algorithm 2, versus iteration number are shown respectively in Fig. 10 and 11.

It can be seen that the EGO algorithm can find the converged solution with different starting sample sets. At the final iteration, the maximum of expected improvement $max(EI(\mathbf{x}))$ is sufficiently small, which guarantee the precision of the solution.

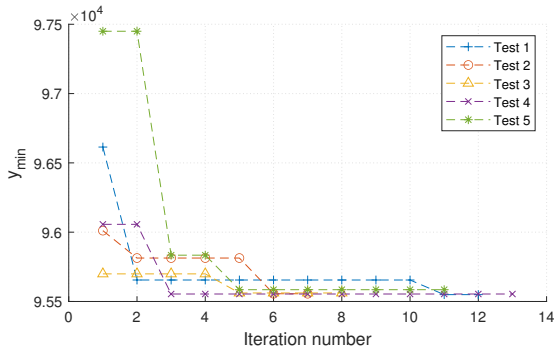
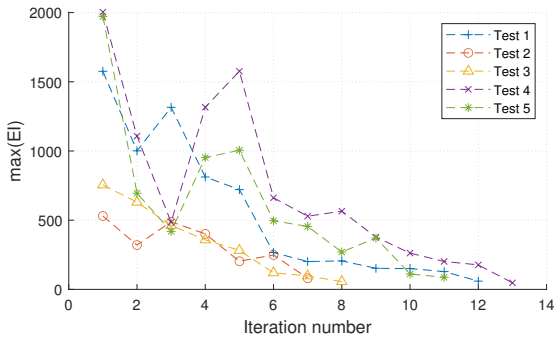
Concerning the computing time, the optimal sizing option is found with less than 14 iterations. Together with the 10 starting samples, the function evaluation runs are limited to less than 24 times. Compared to the extensive search, the EGO is much more efficient computationally. In this scenario, the computing



(a) Kriging function surface and samples in design set.



(b) Expected improvement.

Fig. 9. Final Kriging function surface and EI .Fig. 10. y_{min} evolution with iteration number.Fig. 11. $max(EI)$ evolution with iteration number.

time with the proposed bi-level optimization is approximately

30 mins.

In the solution, the optimal numbers of PV panels and WTs are respectively 66 and 5. Correspondingly, $C_g = 9.559 \times 10^4$ €, in which $C_s = 4.624 \times 10^4$ € and $C_e = 4.935 \times 10^4$ €. It is observed the electricity consumption is reduced significantly thanks to more PV and WT installations, as well as load scheduling operation. Even though the system cost is higher, the total cost is reduced regarding the last two scenarios.

The generation and consumption powers of the specific production cycle are shown in Fig. 12. Comparing to the case shown in Fig. 6, more energy is generated since the system size is bigger. In addition, the local generation could almost cover the energy consumption during the production cycle, which contributes to reduce the electricity cost from the grid.

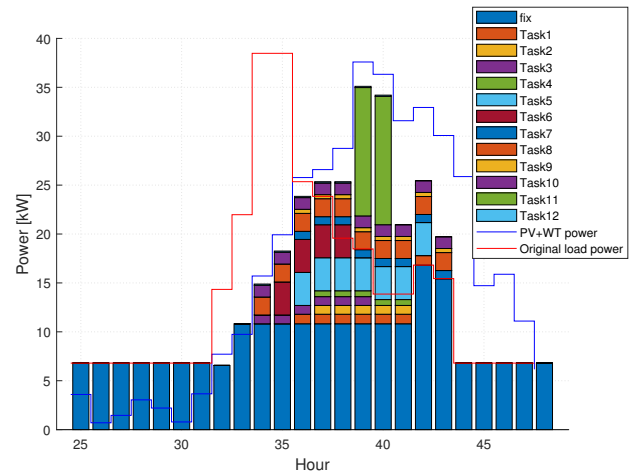


Fig. 12. Comparison of the generated power and load power with optimally sized system. Red line: original load power; Blue line: generated power; Colourful blocks: scheduled power.

E. Scenario 4: system sizing with energy storage without load scheduling

The installation of ESUs is a more regular solution to overcome the power generation and consumption mismatch and use renewable energy more sufficiently. For comparison, the sizing of the hybrid energy system with energy storage installation is studied in this scenario. The energy flow management in the hybrid energy system is described in Section II. For each sizing option (combination of the PV panel, WT and battery numbers), the system cost C_s can be calculated through (7). The power supplied by utility grid P_g during the concerned period can be deduced through Algorithm 1 and the electricity cost C_e can then be calculated with (12) and (15). An exhaustive research is used in this case to seek for the optimal combination of the PV panel, WT and battery numbers.

The optimal numbers of PV panels, WTs and batteries are found to be respectively 48, 4 and 3. C_g is 1.006×10^5 €, in which $C_s = 3.863 \times 10^4$ € and $C_e = 6.199 \times 10^4$ €. Compared with the system design without energy storage installation (scenario 1), the global cost is reduced slightly due to the decrease in electricity cost. However, the benefit of

energy storage installation is not evident because additional cost from batteries is also introduced. The output power of the local energy system (bar plot) and the load power of a selected workday are shown in Fig. 13. It can be seen that the generated power from PV and WT is more than the load power from 38 h to 47 h. The excess part is stored in the installed battery packs. However, between 25 h and 35 h, even the generated power is less than the required power, the batteries cannot compensate the power loss due to the limits of SOC and output power.

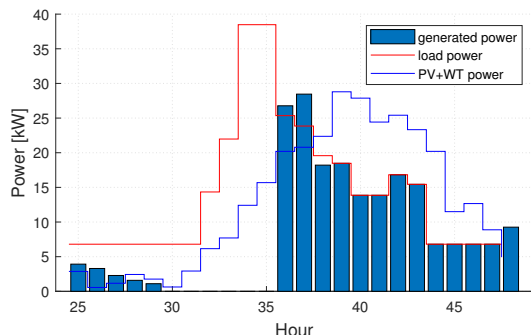


Fig. 13. Generated and load powers of the system with energy storage.

F. Results synthesis and discussion

The optimal sizing results and the corresponding costs for the four scenarios are summarized in Table IV. Regarding the global cost, the system design considering load scheduling (scenario 3) achieves the best performance. The energy storage installation (scenario 4) is not so beneficial. The system with energy storage can only reduce a little global cost compared to the pure PV/WT system without energy storage (scenario 1). The post scheduling with a pre-designed pure PV/WT (scenario 2) can be even more beneficial. It can therefore be interesting to schedule the loads to obtain equivalent effect as energy storage installation.

In the studied production cycle, the starting time hour k_{start} and the end time hour k_{end} of the involved tasks are constrained by staffs' working time. The scheduling flexibility is therefore limited. For comparison, the costs are calculated in scenario 2 and 3 when the k_{start} and k_{end} are set respectively at 1 and 24, which means that the different tasks can be scheduled during one production period without time constraints. The corresponding results are shown in Table IV. It can be seen that the benefits in the two scenarios are both improved significantly. It can be further deduced that the proposed approach could be more interesting for the users with more flexible working time.

It should also be noted that the sizing result is case-dependent. The benefit of the proposed bi-level optimization sizing method varies with both energy generation and load patterns. For instance, the proposed bi-level optimization sizing method could be less beneficial in the cases where the proportion of controllable load is relatively small.

This study has put its importance on the impact of load scheduling flexibility on system sizing. The prediction of

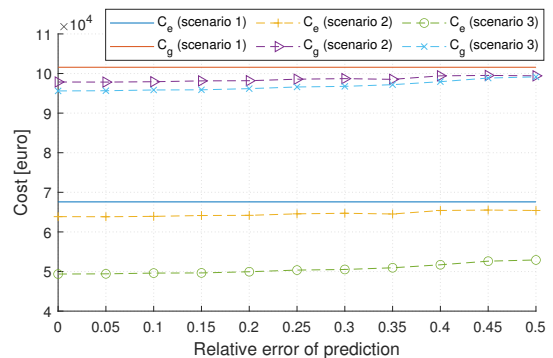


Fig. 14. Variations of costs versus relative error of the prediction of power generation in scenario 2 and 3.

power generation has an important impact on the performance of the proposed strategy since the power generation used for load scheduling is predicted in practice.

Previous results are obtained assuming that the power generation can be precisely predicted. To evaluate the effect of the power generation prediction, errors at different levels are incorporated into the power generation used for the load scheduling in scenario 2 and 3. The electricity costs (C_e) and total costs (C_g) under different relative error levels are calculated and shown in Fig. 14. It can be seen that the benefit of load scheduling in saving electricity cost and the total cost decreases with the increase of the prediction error. It can also be observed that it is beneficial to integrate the load scheduling operation even the relative error of the prediction reaches 50%. Comparing the results in scenario 2 and 3, it is beneficial to integrate the load scheduling in the sizing phase. However, the superiority of scenario 3 declines when the prediction error increases. The performance of the prediction of renewable energy generation is therefore important to the proposed sizing strategy.

An industrial energy use is concerned in this work. The peak load power in the studied case is of tens kW. To fulfil the energy storage requirement, numerous battery needs to be installed in scenario 4, which is not economically beneficial. Other more economical energy storage solutions could be more interesting for industrial loads. With a proper energy storage design, it could even more beneficial when the energy flow is managed considering both energy generation and consumption sides. However, a more complicated optimization problem might have to be solved.

In this study, it is considered that the different controllable tasks are independent in the production cycle. In a more general industrial case, the interdependent, sequential and mutual exclusive tasks should also be taken into consideration in the load model. Accordingly, the resolution method could also be adapted to the new model formulation.

In the studied case, the locally generated energy is not allowed to flow to the utility power grid. For instance, in Fig. 12, the surplus energy between 16 h and 24 h will generally be wasted. The surplus energy could account for an important part. This could explain that the benefit of installing more PV panels and WTs in scenario 3 is not so evident.

TABLE IV
SIZINGS AND COSTS IN DIFFERENT SCENARIOS

Scenario	k_{start}, k_{end}	N_{pv}, N_{wt}, N_{bat}	System cost (€)	Electricity cost (€)	Total cost (€)
1	null	44, 4, 0	3.400×10^4	6.758×10^4	1.016×10^5
2	7,20	44, 4, 0	3.400×10^4	6.385×10^4	9.785×10^4
2 (comparison group)	1,24	44, 4, 0	3.400×10^4	5.806×10^4	9.206×10^4
3	7,20	66, 5, 0	4.624×10^4	4.935×10^4	9.559×10^4
3 (comparison group)	1,24	41, 6, 0	4.250×10^4	4.691×10^4	8.941×10^4
4	null	48, 4, 3	3.863×10^4	6.199×10^4	1.006×10^5

In this study, the electricity price is assumed to be constant as its practical yearly variation is hard to quantify. The electricity price value does not affect the down-level optimization dedicated to load scheduling regarding (14). The sizing result is nevertheless related to the electricity price regarding (15) and (16). More specifically, when the electricity price is lower, the benefit of local energy system installation will also be lower.

VI. CONCLUSION

An optimal sizing approach is proposed for grid-connected hybrid energy systems possessing load scheduling capacity. To achieve load scheduling, the local power model is built as a function of starting times of individual tasks. A bi-level optimization formulation is proposed to combine load scheduling with the system sizing approach. GA and EGO algorithms are respectively used for the two levels.

From the results of a real case study, it can be concluded that the electricity consumed from the power grid can be reduced thanks to the load scheduling action, given the same local energy generation. In the studied case, it is demonstrated that the load scheduling operation could be more economically beneficial than energy storage installation. Moreover, by integrating the load scheduling into the system design phase, the renewable energy consumption capacity of locally generated energy is enhanced. It is therefore motivated to install more renewable energy units to compensate the local consumption with load scheduling capability.

In the ongoing work, efforts are being taken to integrate an interactive dynamic electricity pricing model and an energy generation prediction model into the load scheduling process. The sizing strategy is also being tested for other types of electricity consumer with load flexibility.

REFERENCES

- [1] N. I. Nwulu and X. Xia, "Optimal dispatch for a microgrid incorporating renewables and demand response," *Renewable Energy*, vol. 101, pp. 16–28, 2017.
- [2] Y. Yoldaş, A. Önen, S. Mueyen, A. V. Vasilakos, and İrfan Alan, "Enhancing smart grid with microgrids: Challenges and opportunities," *Renewable and Sustainable Energy Reviews*, vol. 72, pp. 205–214, 2017.
- [3] A. S. Ogunjuyigbe, T. R. Ayodele, and O. A. Akinola, "Optimal allocation and sizing of PV/Wind/Split-diesel/Battery hybrid energy system for minimizing life cycle cost, carbon emission and dump energy of remote residential building," *Applied Energy*, vol. 171, pp. 153–171, 2016.
- [4] S. Upadhyay and M. P. Sharma, "A review on configurations, control and sizing methodologies of hybrid energy systems," *Renewable and Sustainable Energy Reviews*, vol. 38, pp. 47–63, 2014.
- [5] K. Anoune, M. Bouya, A. Astito, and A. B. Abdellah, "Sizing methods and optimization techniques for PV-wind based hybrid renewable energy system: A review," *Renewable and Sustainable Energy Reviews*, vol. 93, no. April, pp. 652–673, 2018. [Online]. Available: <https://doi.org/10.1016/j.rser.2018.05.032>
- [6] F. A. Khan, N. Pal, and S. H. Saeed, "Review of solar photovoltaic and wind hybrid energy systems for sizing strategies optimization techniques and cost analysis methodologies," *Renewable and Sustainable Energy Reviews*, vol. 92, no. April, pp. 937–947, 2018. [Online]. Available: <https://doi.org/10.1016/j.rser.2018.04.107>
- [7] J. Lian, Y. Zhang, C. Ma, Y. Yang, and E. Chaima, "A review on recent sizing methodologies of hybrid renewable energy systems," *Energy Conversion and Management*, vol. 199, no. September, p. 112027, 2019. [Online]. Available: <https://doi.org/10.1016/j.enconman.2019.112027>
- [8] H. Demolli, A. S. Dokuz, A. Ecemis, and M. Gokcek, "Location-based optimal sizing of hybrid renewable energy systems using deterministic and heuristic algorithms," *International Journal of Energy Research*, vol. 45, no. 11, pp. 16 155–16 175, 2021.
- [9] A. Askarzadeh and L. dos Santos Coelho, "A novel framework for optimization of a grid independent hybrid renewable energy system: A case study of Iran," *Solar Energy*, vol. 112, pp. 383–396, 2015. [Online]. Available: <http://dx.doi.org/10.1016/j.solener.2014.12.013>
- [10] A. Maleki and A. Askarzadeh, "Artificial bee swarm optimization for optimum sizing of a stand-alone pv/wt/fc hybrid system considering lpsp concept," *Solar Energy*, vol. 107, pp. 227–235, 2014. [Online]. Available: <https://www.sciencedirect.com/science/article/pii/S0038092X1400245X>
- [11] S. Barakat, H. Ibrahim, and A. A. Elbaset, "Multi-objective optimization of grid-connected pv-wind hybrid system considering reliability, cost, and environmental aspects," *Sustainable Cities and Society*, vol. 60, p. 102178, 2020. [Online]. Available: <https://www.sciencedirect.com/science/article/pii/S2210670720301657>
- [12] B. K. Das, R. Hassan, M. S. H. Tushar, F. Zaman, M. Hasan, and P. Das, "Techno-economic and environmental assessment of a hybrid renewable energy system using multi-objective genetic algorithm: A case study for remote island in bangladesh," *Energy Conversion and Management*, vol. 230, p. 113823, 2021.
- [13] M. Fadaee and M. A. Radzi, "Multi-objective optimization of a stand-alone hybrid renewable energy system by using evolutionary algorithms: A review," *Renewable and Sustainable Energy Reviews*, vol. 16, no. 5, pp. 3364–3369, 2012. [Online]. Available: <http://dx.doi.org/10.1016/j.rser.2012.02.071>
- [14] S. Kim, K. Cho, J. Kim, and G. Byeon, "Field study on operational performance and economics of lithium-polymer and lead-acid battery systems for consumer load management," *Renewable and Sustainable Energy Reviews*, vol. 113, p. 109234, 2019.
- [15] R. Atia and N. Yamada, "Sizing and Analysis of Renewable Energy and Battery Systems in Residential Microgrids," *IEEE Transactions on Smart Grid*, vol. 7, no. 3, pp. 1204–1213, 2016.
- [16] A. A. Almezhizia, H. M. K. Al-Masri, and M. Ehsani, "Integration of renewable energy sources by load shifting and utilizing value storage," *IEEE Transactions on Smart Grid*, vol. 10, no. 5, pp. 4974–4984, 2019.
- [17] Z. Zhao, W. C. Lee, Y. Shin, and K.-B. Song, "An optimal power scheduling method for demand response in home energy management system," *IEEE Transactions on Smart Grid*, vol. 4, no. 3, pp. 1391–1400, 2013.
- [18] F. Mangiatordi, E. Pallotti, P. Del Vecchio, and F. Leccese, "Power consumption scheduling for residential buildings," in *2012 11th Interna-*

- tional Conference on Environment and Electrical Engineering.* IEEE, 2012, pp. 926–930.
- [19] L. Gelazanskas and K. A. Gamage, “Demand side management in smart grid: A review and proposals for future direction,” *Sustainable Cities and Society*, vol. 11, pp. 22 – 30, 2014.
- [20] M. Behrangrad, “A review of demand side management business models in the electricity market,” *Renewable and Sustainable Energy Reviews*, vol. 47, pp. 270–283, 2015.
- [21] E. Guelpa and V. Verda, “Demand response and other demand side management techniques for district heating: A review,” *Energy*, vol. 219, p. 119440, 2021.
- [22] Z. Wu, H. Tazvinga, and X. Xia, “Demand side management of photovoltaic-battery hybrid system,” *Applied Energy*, vol. 148, pp. 294–304, 2015.
- [23] Z. Wang, F. Gao, Q. Zhai, X. Guan, J. Wu, and K. Liu, “Electrical load tracking analysis for demand response in energy intensive enterprise,” *IEEE Transactions on Smart Grid*, vol. 4, no. 4, pp. 1917–1927, 2013.
- [24] M. Saidi, Z. Li, S. B. Elghali, and R. Outbib, “Optimal sizing of hybrid grid-connected energy system with demand side scheduling,” in *IECON 2019-45th Annual Conference of the IEEE Industrial Electronics Society*, vol. 1. IEEE, 2019, pp. 2209–2214.
- [25] A. Kaabeche, M. Belhamel, and R. Ibtiouen, “Techno-economic valuation and optimization of integrated photovoltaic/wind energy conversion system,” *Solar energy*, vol. 85, no. 10, pp. 2407–2420, 2011.
- [26] T. Wu, Q. Yang, Z. Bao, and W. Yan, “Coordinated energy dispatching in microgrid with wind power generation and plug-in electric vehicles,” *IEEE Transactions on Smart Grid*, vol. 4, no. 3, pp. 1453–1463, 2013.
- [27] R. L. Haupt, “Antenna design with a mixed integer genetic algorithm,” *IEEE Transactions on Antennas and Propagation*, vol. 55, no. 3, pp. 577–582, 2007.
- [28] J. D. Foster, A. M. Berry, N. Boland, and H. Waterer, “Comparison of mixed-integer programming and genetic algorithm methods for distributed generation planning,” *IEEE transactions on power systems*, vol. 29, no. 2, pp. 833–843, 2013.
- [29] K. Deep, K. Pratap, M. L. Kansal, and C. Mohan, “A real coded genetic algorithm for solving integer and mixed integer optimization problems,” *Applied Mathematics and Computation*, vol. 212, no. 2, pp. 505–518, 2009.
- [30] “Matlab mixed integer ga optimization example,” <https://www.mathworks.com/help/gads/mixed-integer-optimization.html>, accessed: 2021-04-01.
- [31] D. R. Jones, M. Schonlau, and W. J. Welch, “Efficient global optimization of expensive black-box functions,” *Journal of Global optimization*, vol. 13, no. 4, pp. 455–492, 1998.
- [32] D. Zhan, J. Qian, and Y. Cheng, “Pseudo expected improvement criterion for parallel EGO algorithm,” *Journal of Global Optimization*, vol. 68, no. 3, pp. 641–662, 2017.
- [33] R. Rigo-Mariani, B. Sareni, and X. Roboam, “Integrated optimal design of a smart microgrid with storage,” *IEEE Transactions on Smart Grid*, vol. 8, no. 4, pp. 1762–1770, 2015.